applied optics

Generation of a frequency-quadrupled phase-coded signal using optical carrier phase shifting and balanced detection

Xuan Li,[1,2] Shanghong Zhao,[1,*] Shilong Pan,[2] Zihang Zhu,[1] Kun Qu,[1] and Tao Lin[1]

[1]Information and Navigation College, Air Force Engineering University, Xian 710077, China
[2]Key Laboratory of Radar Imaging and Microwave Photonics, Ministry of Education, Nanjing University of Aeronautics and Astronautics, Nanjing 210016, China
*Corresponding author: zhaoshangh@aliyun.com

Received 11 November 2016; revised 23 December 2016; accepted 2 January 2017; posted 5 January 2017 (Doc. ID 280675); published 1 February 2017

A novel approach for photonic generation of a frequency-quadrupled phase-coded signal using optical carrier shifting and balanced detection is proposed and demonstrated. The key component of the scheme is an integrated dual-polarization quadrature phase shift-keying (DP-QPSK) modulator. In the modulator, an RF signal is applied to the upper QPSK modulator to generate high-order optical sidebands, while an electrical coding signal is applied to the bottom QPSK modulator to perform optical carrier phase shifting. After that, a frequency-quadrupled phase-coded signal with an exact π-phase shift is generated through balanced detection. The proposed scheme has a simple, compact structure and good tunability. Besides, a phase-coded pulse can be directly obtained when a three-level rectangular coding signal is applied. A proof-of-concept experiment is carried out. The generation of a 2-Gbit/s phase-coded signal with a frequency tuning from 12.12 to 28 GHz is experimentally demonstrated, and the generation of a phase-coded microwave pulse is also verified.

OCIS codes: (060.4080) Modulation; (060.5625) Radio frequency photonics; (280.5600) Radar; (350.4010) Microwaves.

https://doi.org/10.1364/AO.56.001151

1. INTRODUCTION

Phase-coded microwave or millimeter signals have wide applications in modern radar and communication systems. As a result of the extreme congestion of low-frequency bands of the RF spectrum, the operation frequency of phase-coded signal is developing toward high-frequency bands [1]. Conventionally, a phase-coded signal is generated in the electrical domain, but it suffers from limited operation bandwidth and small tunability due to the inherent electronic bottleneck. To deal with these problems, photonic methods have been proposed to generate a phase-coded signal thanks to the advantages of photonic techniques such as broad bandwidth, good tunability, and immunity to electromagnetic interference.

Numerous photonic techniques have been proposed to generate a phase-coded signal. For example, an ultrashort optical pulse-shaping technique can be used to generate a phase-coded signal with high frequency and wide bandwidth by using either spectral shaping followed by frequency-to-time mapping method [2,3] or direct space-to-time mapping method [4]. However, the time duration of the generated phase-coded pulse is usually limited (<1 μs), which may hinder its applications. To generate a phase-coded signal with long time duration, the phase modulation technique can be employed [5–7]. In this method, two optical sidebands are first generated by driving an RF signal to a modulator. Then the two sidebands are separated by a wavelength-selective device. Finally, an electrical coding signal is applied to a phase modulator to modulate with one of the sidebands. After optical to electrical conversion, a phase-coded signal with high frequency and a long time duration can be generated. The main drawback of this method is that the two optical paths are physically separated and independently processed, which makes the signal suffer severely from environment variations. To improve stability, polarization modulation technique can be utilized, thanks to the complementarily phase-modulation function of the integrated polarization modulator (PolM) [8–13]. However, the schemes based on the polarization modulation are usually complicated and costly due to the use of multiple modulators. A phase-coded signal can also be generated based on the optical carrier phase-shifting technique [14–17]. In this method, a modulator with two parallel branches is usually needed, such as a dual-drive Mach–Zehnder modulator (MZM) [14,15], a quadrature phase shift-keying (QPSK) modulator [16], or a dual-polarization integrated modulator [17]. In the modulator, one branch is

driven by an RF signal to generate two optical sidebands with the optical carrier suppressed, while another branch is driven by a coding signal to control the phase shift of the optical carrier. When the phase shift introduced by the coding signal is π, a phase-coded microwave signal can be obtained after square-law detection. The key advantage of this method is the compact and simple structure due to the use of only one modulator. However, the frequency of the generated phase-coded signal is limited by the bandwidth of the modulator (typically less than 40 GHz), as there is no frequency-multiplied operation in the phase-coding operation.

To overcome the frequency restriction caused by the bandwidth of the modulator or electrical devices, frequency-multiplication technique is highly desired at the time of generating a high-frequency phase-coded signal. Previously, a frequency-doubled phase-coded signal was generated [7,11,12], but the frequency multiplication factor is small, which can hardly support high-frequency applications. The generation of a frequency-quadrupled phase-coded signal has also been proposed [8], but the polarization maintaining fiber Bragg grating (FBG) used in the scheme is wavelength and polarization dependent, making the frequency tuning range very limited. Recently, we demonstrated a frequency-quadrupled phase-coded signal generator with large tunability based on an FBG-incorporated Sagnac loop and a PolM [13]. Again, the system is complicated because the polarization modulation technique is employed.

In this paper, we propose and experimentally demonstrate a scheme to generate a frequency-quadrupled phase-coded signal by using optical carrier phase shifting and balanced detection techniques. Compared with the previous frequency-multiplied phase-coded signal generators, the proposed scheme has a simple and compact structure due to the use of only one integrated modulator. At the same time, the scheme can meet the requirement of high-frequency applications because of the frequency-quadrupled operation, and provide an ultrawide frequency tuning range, as no wavelength-dependent device is involved. In addition, the generated phase-coded pulse is free from background noise and higher-order distortion thanks to the balanced detection. Last but not least, the approach is possible to generate not only a continuous wave (CW) phase-coded signal but also a phase-coded pulse, which makes the scheme directly applicable in pulse-radar systems without using an additional optical intensity modulator to truncate a CW signal into a pulse.

2. PRINCIPLE

Figure 1 shows the schematic diagram of the proposed frequency-quadrupled phase-coded signal generator. The key component of the scheme is a dual-polarization QPSK (DP-QPSK) modulator, which is an integrated device including a 3-dB optical coupler, two parallel QPSK modulators, and a polarization beam combiner (PBC). Each of the QPSK modulators consists of two subMZMs placed in a main MZM. In the scheme, a linearly polarized light from a laser diode (LD) is sent to the DP-QPSK modulator with its polarization state adjusted by a polarization controller (PC1). In the modulator, the light is equally split into two branches, modulated by two electrical driving signals of the two QPSK modulators,

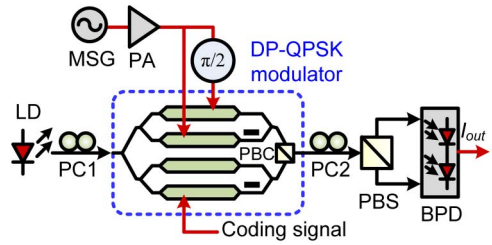

Fig. 1. Schematic diagram of the proposed phase-coded signal generator.

respectively, and then combined through the PBC with orthogonal polarization states. An RF driving signal from a microwave signal generator (MSG) is amplified by an electrical power amplifier (PA), and then divided into two paths and applied to the two RF input ports of the upper QPSK modulator. In one of the paths, an electrical phase shifter is inserted to introduce a phase difference of $\pi/2$ between the two RF signals. When both the subMZMs and the main MZM of the upper QPSK modulator are biased at the maximum transmission point, the optical signal at the output of this modulator can be expressed as [18]

$$\begin{aligned} E_{\text{up}}(t) &= \frac{\sqrt{2}}{8}E_0\,\exp(j\omega_c t) \\ &\quad\times\begin{bmatrix}\exp(jm\,\sin\,\omega t)+\exp(-jm\,\sin\,\omega t)\\ +\exp(jm\,\cos\,\omega t)+\exp(-jm\,\cos\,\omega t)\end{bmatrix} \\ &= \frac{\sqrt{2}}{8}E_0\,\exp(j\omega_c t)\sum_{n=-\infty}^{\infty}[J_n(m)+J_n(-m)](1+j^n) \\ &\quad\times\exp(jn\omega t) \\ &= \frac{\sqrt{2}}{2}E_0\,\exp(j\omega_c t)\sum_{n=-\infty}^{\infty}J_{4n}(m)\,\exp(j4n\omega t), \end{aligned} \tag{1}$$

where the insertion loss of the modulator is neglected. E_0 and ω_c are the amplitude and frequency of the light from the LD, ω is the frequency of the RF signal, m is the modulation index of the upper QPSK modulator, and J_n is the nth-order Bessel function of the first kind. As demonstrated in [18,19], an optical carrier and two fourth-order sidebands are generated through one QPSK modulator. To perform the phase-coding operation, another QPSK modulator should be driven by an electrical coding signal and the balanced detection should be employed.

In the bottom QPSK modulator, both the subMZMs are biased at the minimum transmission point and the main MZM is biased at the maximum transmission point, and one of the subMZMs is driven by an electrical coding signal. The output optical signal of this QPSK modulator can be written as

$$\begin{aligned} E_{\text{bott}}(t) &= \frac{\sqrt{2}}{8}E_0\,\exp(j\omega_c t) \\ &\quad\times\begin{bmatrix}\exp\left(j\beta s(t)+j\frac{\pi}{2}\right)+\exp\left(-j\beta s(t)-j\frac{\pi}{2}\right)\\ +\exp\left(j\frac{\pi}{2}\right)+\exp\left(-j\frac{\pi}{2}\right)\end{bmatrix} \\ &= -\frac{\sqrt{2}}{4}E_0\,\sin[\beta s(t)]\exp(j\omega_c t), \end{aligned} \tag{2}$$

where β is the modulation index of the modulator and $s(t)$ is the normalized waveform of the coding signal.

The two modulated optical signals are combined by the PBC with orthogonal polarization states. The optical signal output from the DP-QPSK modulator is then sent to a polarization beam splitter (PBS) through another PC (PC2). By tuning PC2 to make the polarization state of E_{up} or E_{bott} has an angle of 45° to one principal axis of the PBS; the two optical signals from two output ports of the PBS are given by

$$E_{1,2}(t) = \frac{1}{2}[E_{\text{up}}(t) \pm E_{\text{bott}}(t)]. \quad (3)$$

Then the two optical signals are sent to a balanced photodetector (BPD). The generated electrical signal at one PD of the BPD (i.e., PD1) is

$$I_1(t) = R[E_1(t)E_1^*(t)] = \frac{R}{8}E_0^2\left\{\begin{array}{l}[J_0(m) + 2J_4(m)\cos 4\omega t]^2 + \frac{1}{4}[\sin \beta s(t)]^2 \\ -[J_0(m) + 2J_4(m)\cos 4\omega t]\sin[\beta s(t)]\end{array}\right\}, \quad (4)$$

where R is the responsivity of PD1 and * denotes conjugation.

The electrical signal at the output of the BPD is

$$I_{\text{out}}(t) = I_1(t) - I_2(t) = -\frac{R}{4}E_0^2[J_0(m) + 2J_4(m)\cos 4\omega t]\sin[\beta s(t)]. \quad (5)$$

As can be seen from Eqs. (4) and (5), the DC component and the harmonics with frequency of 4ω and 8ω are removed, thanks to the balanced detection. A signal at frequency of 4ω with its sign determined by $\sin[\beta s(t)]$ is generated. It should be noted that a baseband modulation is also obtained as the term of $J_0(m)\sin[\beta s(t)]$. Considering that the baseband component cannot be radiated to free space due to the bandpass nature of the transmitting antenna, it can be easily eliminated.

Assuming that the electrical coding signal is a binary signal with bits "−1" and "+1," then the generated electrical signal at the output of the BPD is modified as

$$I_{\text{out}}(t) = \left\{\begin{array}{ll} -\frac{R}{2}\sin \beta E_0^2 J_4(m)\cos 4\omega t & s(t) = -1 \\ \frac{R}{2}\sin \beta E_0^2 J_4(m)\cos 4\omega t & s(t) = +1 \end{array}\right. . \quad (6)$$

Therefore, a phase-coded microwave signal with a precise π phase difference at frequency of 4ω is generated.

Furthermore, when the coding signal is a three-level rectangular coding signal, a phase-coded pulse can be obtained. The generated pulse is

$$I_{\text{out}}(t) = \left\{\begin{array}{ll} -\frac{R}{2}\sin \beta E_0^2 J_4(m)\cos 4\omega t & s(t) = -1 \\ 0 & s(t) = 0 \\ \frac{R}{2}\sin \beta E_0^2 J_4(m)\cos 4\omega t & s(t) = +1 \end{array}\right. , \quad (7)$$

where 0 stands for no voltage, and −1 or +1 represents the sign of the voltage of the coding signal. As a result, a frequency-quadrupled phase-coded pulse can be easily generated by applying a three-level coding signal to the modulator. If the voltage is 0, there is no output signal; otherwise, a pulse would appear, and the phase of the microwave pulse can be switched between 0 and π according to the sign of the voltage of the coding signal.

3. EXPERIMENT RESULTS AND DISCUSSIONS

A proof-of-concept experiment is carried out based on the setup shown in Fig. 1. A CW light is generated from an LD (Agilent N7714A) with a wavelength of 1552.504 nm and a power of 13 dBm. The modulator is a commercially available DP-QPSK modulator (Fujitsu FTM7977HQA) which has a 3-dB bandwidth of ~23 GHz. An RF signal generated from an MSG (Agilent E8257D) is preamplified by an electrical PA (Agilent 83020A) that has a maximum output power of 30 dBm. The coding signal is provided by a pulse pattern generator (PPG) (Anritsu MP1763C) that has an operation frequency from 0.05 to 12.5 GHz. The optical to electrical conversion is performed by a 40-GHz BPD (u^2t BPDV2150R). The optical and electrical signals are measured by an optical spectrum analyzer (Yokogawa AQ6370C) with a resolution of 0.02 nm and a digital storage oscilloscope (Agilent DSO-X 92504A) with a sampling rate of 80 GS/s, respectively.

First, the MSG is tuned to 3.03 GHz. The MZMs in the upper QPSK modulator are DC-biased to generate optical carrier and fourth-order sidebands. Figure 2 shows the measured optical spectra of the generated signals. The black line represents the output optical spectrum of the DP-QPSK modulator. It can be seen that the optical carrier and two fourth-order sidebands are obtained. Due to the finite extinction ratio of the modulator (22 dB for the main MZMs and 20 dB for the subMZMs), the other sidebands also appear, and the optical spurious suppression ratio is 15 dB. By adjusting PC2, the optical signals from upper and bottom QPSK modulators can be separated from the PBS, as shown in the figure, in which the red line and the blue dashed line represent the optical spectra from the two ports of the PBS, respectively. Due to the finite polarization extinction ratio of the PBS, the fourth-order sidebands still exist in port 2, but the powers are suppressed 32 dB by the polarization selection.

Then the DC bias points of the two subMZMs in the bottom QPSK modulator are adjusted to suppress the optical carrier of port 2 of the PBS. After that, a 2-Gbit/s 13-bit Barker coding signal with a pattern of "+1 + 1 + 1 + 1 + 1− 1 − 1 + 1 + 1 − 1 + 1 − 1 + 1" is applied to one subMZM. An erbium-doped fiber amplifier (EDFA) is followed by the modulator to boost the optical power. By adjusting PC2, a frequency-quadrupled phase-coded signal is generated through

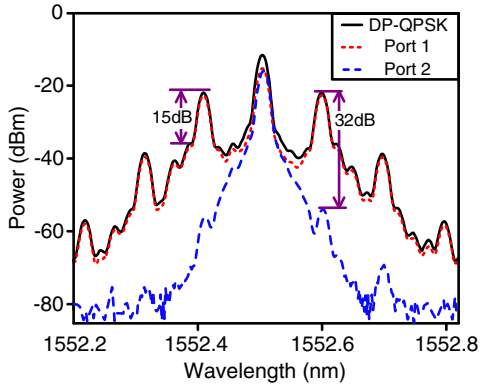

Fig. 2. Measured spectra of the optical signal output from the DP-QPSK modulator and the signals split by the PBS.

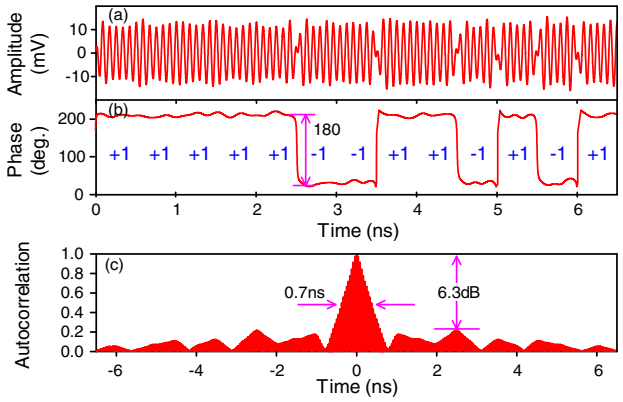

Fig. 3. (a) Waveform of the 2-Gbit/s 12.12-GHz phase-coded signal, (b) the extracted phase shift, and (c) the autocorrelation of the generated signal.

the BPD. To eliminate the electrical spurious components caused by the optical spurious sidebands and the electrical baseband signal, a bandpass filter is placed after the BPD. Figure 3(a) shows the waveform of the generated 2-Gbit/s 12.12-GHz phase-coded signal with a time duration of 6.5 ns. Figure 3(b) shows the phase shift extracted from the generated signal, a phase difference of π is obviously observed between bit "+1" and bit "−1." The pulse-compression capability of the generated phase-coded signal is also investigated. Figure 3(c) shows the autocorrelation of the generated 6.5 ns signal. The main-to-sidelobe ratio (MSR) is 6.3 dB, and the full width at half-maximum (FWHM) of the compressed pulse is 0.7 ns. Thus, a compression ratio of 9.3 is achieved.

To investigate the frequency tunability, the MSG is tuned to 5 GHz. Figures 4(a) and 4(b) show the waveform of the 2-Gbit/s phase-coded signal with a frequency of 20 GHz and the corresponding extracted phase shift. In another study, the MSG is adjusted to 7 GHz. The generated phase-coded signal and the corresponding extracted phase shift are shown in Figs. 4(c) and 4(d), respectively. Figures 5(a) and 5(b) show the autocorrelations of the generated 20-GHz and 28-GHz

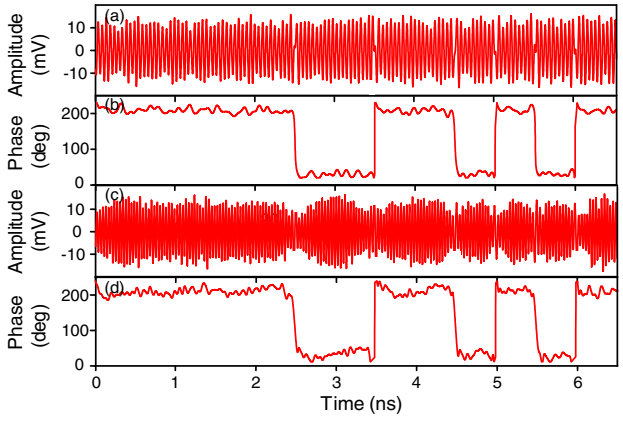

Fig. 4. (a) Waveform and (b) the extracted phase shift of the 2-Gbit/s 20-GHz phase-coded signal, (c) the waveform, and (d) the extracted phase shift of the 2-Gbit/s 28-GHz phase-coded signal.

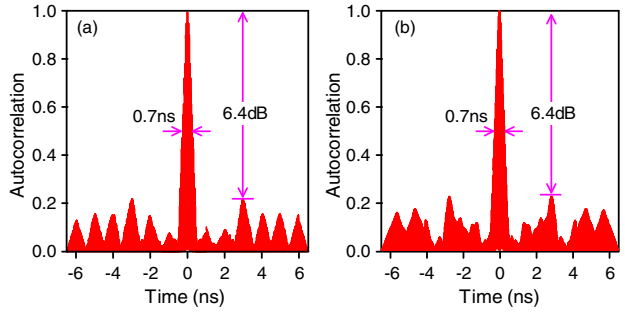

Fig. 5. Autocorrelation of the generated (a) 20-GHz and (b) 28-GHz phase-coded pulses.

phase-coded signals; as can be seen, the FWHM of the two compressed signals are both 0.7 ns, and the MSRs are both 6.4 dB, meaning that the scheme has good frequency tunability and performance stability. Thanks to the frequency-quadrupled operation, a phased-coded signal with a continuous frequency tuning range as large as 92 GHz can be generated by using this DP-QPSK modulator, but a higher frequency cannot be observed in the experiment because the maximum frequency of the oscilloscope is only 32 GHz.

To demonstrate the capability to generate a microwave pulse, the MSG is tuned to 3.03 GHz, and the PPG is defined to output a 2-Gbit/s 36-bit coding signal with a fixed pattern (i.e., 4-bit "1" plus 8-bit "0"). Figure 6(a) shows the measured waveform at the output of the BPD in a time duration of 18 ns; as can be seen, a series of microwave pulses is generated which has a duty cycle of 1/3. The microwave signal is generated with bit "1," and there is no output signal with bit "0." Figure 6(b) shows the zoom in on a single microwave pulse in a time duration of 3 ns. It can be seen that the time cycle of the microwave signal is ∼0.08 ns, which is in accord with the generated 12.12-GHz frequency-quadrupled signal. In the experiment, only a binary coding signal with bits "0" and "1" are used, due to the limitation of the PPG. When a three-level rectangular coding signal is generated and applied to the modulator, a frequency-quadrupled phase-coded microwave pulse with precise phase shift of π can be obtained. Figure 7 shows the simulated results of the generated phase-coded pulse. In the simulation, a three-level rectangular coding signal with 13-bit "0" and 13-bit Barker coding signal $(+1+1+1+1+1-1-1-1-1+1-1+1-1)$ is applied

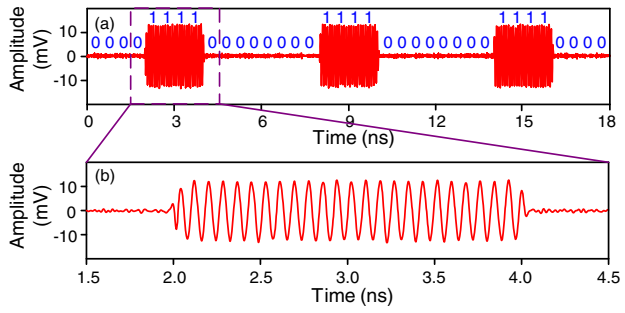

Fig. 6. (a) Measured pulses in a time duration of 18 ns and (b) zoom in on a single 12.12-GHz pulse.

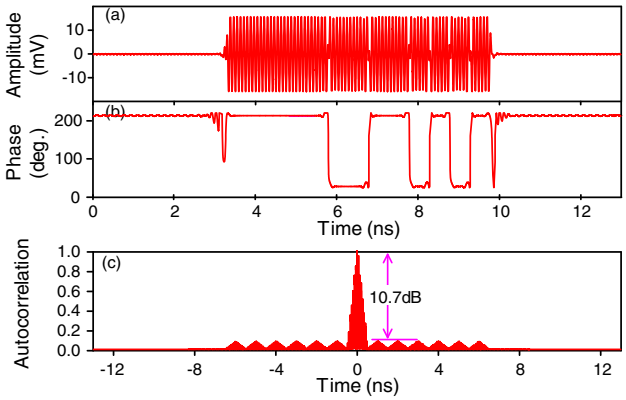

Fig. 7. (a) Simulated 2-Gbit/s 12.12-GHz phase-coded pulse waveform with a time duration of 13 ns, (b) the extracted phase shift, and (c) the autocorrelation of the pulse.

to the modulator. A 6.5-ns phase-coded pulse is obtained in a time duration of 13 ns, as shown in Fig. 7(a), and Fig. 7(b) shows the extracted phase shift from the pulse waveform. It can be seen that the amplitude and the phase envelope of the simulated results are flat, because the parameters in the simulation are set as ideal values, and the noise is neglected. As a result, the pulse compression has a better performance than the experiment result; the MSR of the simulated phase-coded is 10.7 dB, as shown in Fig. 7(c).

The optical loss of the scheme is also investigated. In the experiment, to obtain an electrical waveform with high power after the BPD, the EDFA is set to make each PD have an average input optical power of 10 dBm. The gain of EDFA is about 40 dB, meaning that the total optical loss of the proposed scheme is about 40 dB, which is relatively high when compared with the previously proposed systems [14–17]. The large power consumption has two main origins. The first kind is the insertion loss of the optical components, including 13-dB loss of the modulator and 6-dB loss of the two PCs and the PBS; the insertion loss of the integrated DP-QPSK modulator is larger than the other simple modulators. The second kind is the modulation loss in the modulator, as the modulator is set to obtain the fourth-order optical sidebands; the power consumption is larger than the first-order optical sidebands generation.

One problem associated with the proposed scheme is that the system stability may suffer from the variation of the DC bias points in the modulator. This problem can be resolved by employing a DP-QPSK modulator bias controller (i.e., YY LABS Inc. D0158) in the system.

4. CONCLUSIONS

In conclusion, we have proposed and demonstrated a photonic approach to generate a frequency-quadrupled phase-coded signal based on a DP-QPSK modulator. Because only one integrated modulator is used and there is no optical or electrical filter involved, the system has a simple, compact structure and good frequency tunability. The frequency-quadrupled operation makes the system have a frequency tuning range as large as 92 GHz. The scheme can also be used to directly generate a phase-coded pulse. A 2-Gbit/s phase-coded signal with a frequency tuning from 12.12 to 28 GHz is experimentally generated, and the generation of a phase-coded pulse is also principally verified. The proposed approach can find applications in high-frequency and frequency-agile radar systems and wireless communication systems.

Funding. National Basic Research Program of China (2012CB315705); National Natural Science Foundation of China (NSFC) (61401502, 61422108, 61527820, 61571461).

REFERENCES

1. J. Lin, C. Lu, H. Chuang, F. Kuo, J. Shi, C. Huang, and C. Pan, "Photonic generation and detection of W-Band chirped millimeter-wave pulses for radar," IEEE Photon. Technol. Lett. **24**, 1437–1439 (2012).
2. J. Chou, Y. Han, and B. Jalali, "Adaptive RF-photonic arbitrary waveform generator," IEEE Photon. Technol. Lett. **15**, 581–583 (2003).
3. C. Wang and J. P. Yao, "Phase-coded millimeter-wave waveforms generation using a spatially discrete chirped fiber Bragg grating," IEEE Photon. Technol. Lett. **24**, 1493–1495 (2012).
4. J. D. McKinney, D. E. Leaird, and A. M. Weiner, "Millimeter-wave arbitrary waveform generation with a direct space-to-time pulse shaper," Opt. Lett. **27**, 1345–1347 (2002).
5. H. Jiang, L. Yan, J. Ye, W. Pan, B. Luo, and X. Zou, "Photonic generation of phase-coded microwave signals with tunable carrier frequency," Opt. Lett. **38**, 1361–1363 (2013).
6. Y. Chen, A. Wen, Y. Chen, and X. Wu, "Photonic generation of binary and quaternary phase-coded microwave waveforms with an ultra-wide frequency tunable range," Opt. Express **22**, 15618–15625 (2014).
7. Z. Li, W. Li, H. Chi, X. Zhang, and J. Yao, "Photonic generation of phase-coded microwave signal with large frequency tunability," IEEE Photon. Technol. Lett. **23**, 712–714 (2011).
8. Z. Li, M. Li, H. Chi, X. Zhang, and J. Yao, "Photonic generation of phase-coded millimeter-wave signal with large frequency tunability using a polarization maintaining fiber Bragg grating," IEEE Microw. Wireless Compon. Lett. **21**, 694–696 (2011).
9. L. Wang, W. Li, H. Wang, J. Zheng, J. Li, and N. Zhu, "Photonic generation of phase coded microwave pulses using cascaded polarization modulators," IEEE Photon. Technol. Lett. **25**, 678–681 (2013).
10. Y. Zhang and S. Pan, "Generation of phase-coded microwave signals using a polarization-modulator-based photonic microwave phase shifter," Opt. Lett. **38**, 766–768 (2013).
11. S. Liu, D. Zhu, Z. Wei, and S. Pan, "Photonic generation of widely tunable phase-coded microwave signals based on a dual-parallel polarization modulator," Opt. Lett. **39**, 3958–3961 (2014).
12. Y. M. Zhang, F. Z. Zhang, and S. L. Pan, "Frequency-doubled and phase-coded RF signal generation based on orthogonally polarized carrier-suppressed double sideband modulation," in *Asia Communications and Photonics Conference*, OSA Technical Digest (online) (Optical Society of America, 2014), paper AF3A.2.
13. X. Li, S. Zhao, Y. Zhang, Z. Zhu, and S. Pan, "Generation of a frequency-quadrupled phase-coded signal with large tunability," IEEE Photon. Technol. Lett. **28**, 1980–1983 (2016).
14. Z. Tang, T. Zhang, F. Zhang, and S. Pan, "Photonic generation of a phase-coded microwave signal based on a single dual-drive Mach-Zehnder modulator," Opt. Lett. **38**, 5365–5368 (2013).
15. W. Li, W. Wang, W. Sun, L. Wang, and N. Zhu, "Photonic generation of arbitrarily phase-modulated microwave signals based on a single DDMZM," Opt. Express **22**, 7446–7457 (2014).
16. Y. Yu, J. Dong, F. Jiang, and X. Zhang, "Photonic generation of precisely π phase-coded microwave signal with broadband tunability," IEEE Photon. Technol. Lett. **25**, 1041–1135 (2013).

17. F. Zhang, X. Ge, B. Gao, and S. Pan, "Phase-coded microwave signal generation based on a single electro-optical modulator and its application in accurate distance measurement," Opt. Express **23**, 21867–21874 (2015).
18. X. Li, S. Zhao, Z. Zhu, B. Gong, X. Chu, Y. Li, J. Zhao, and Y. Liu, "An optical millimeter-wave generation scheme based on two parallel dual-parallel Mach-Zehnder modulators and polarization multiplexing," J. Mod. Opt. **62**, 1502–1509 (2015).
19. Y. Gao, A. Wen, W. Jiang, D. Liang, W. Liu, and S. Xiang, "Photonic microwave generation with frequency octupling based on a DP-QPSK modulator," IEEE Photon. Technol. Lett. **27**, 2260–2263 (2015).